Insights into mantle dynamics and thermo-chemical structure through joint inversions of seismic and geodynamic data

- Chang Lu (UT Austin, now Schlumberger)
- Nathan Simmons (LLNL)
- Alessandro Forte (University of Florida)
- Petar Glisovic (UQAM)
- David Rowley (U of Chicago)
- Steve Grand (UT at Austin)

Global Shear Wave Tomography

- Use synthetic seismograms to measure travel time delays relative to a starting model and determine path through mantle by modeling (first order modeling assures correct paths)

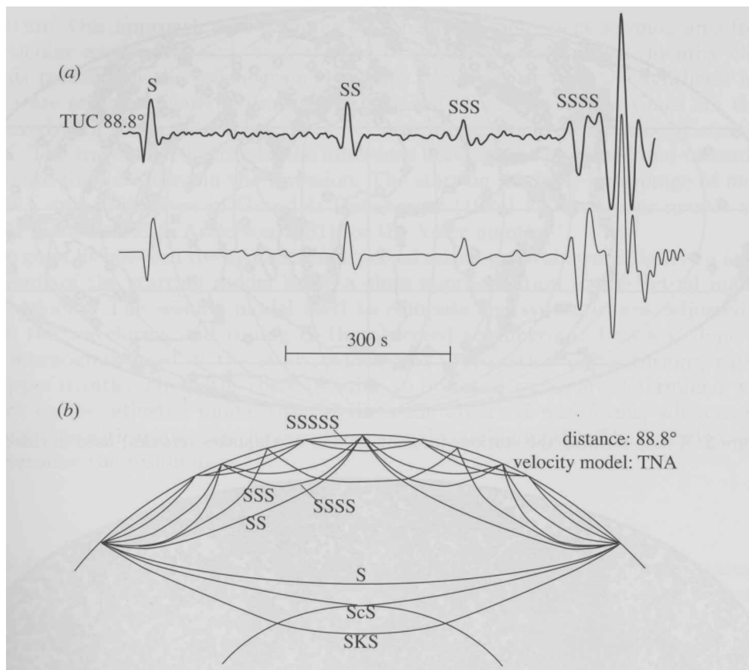

Linear equations relating travel time residuals to perturbations in seismic velocity in blocks

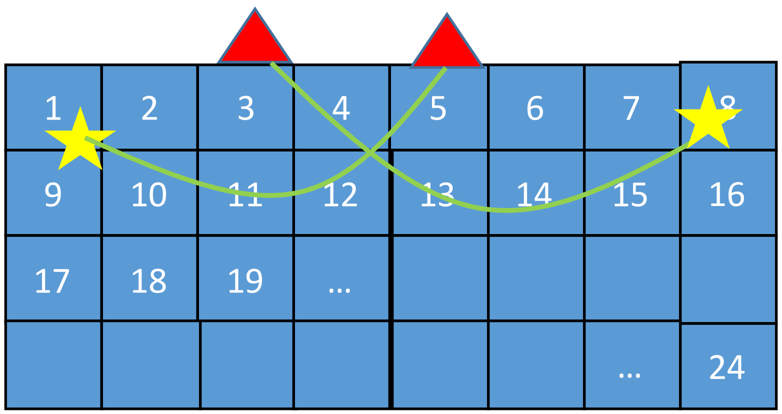

For a given starting velocity model:

- Determine ray path through mantle
- Measure travel time residual relative to the starting model (the difference between predicted time and observed time)
- Parameterize mantle with blocks

Approximate residual:

Ray path length in block i

$$\Delta t = \mathrm{r} = \sum_{i=1}^{N} l_i \left(\Delta \frac{1}{V_i}\right) = \sum_{i=1}^{N} l_i \Delta m_i$$

Velocity in block i

Slowness perturbation in block i

~ 300,000 rays in our model

Also can add in linear equations that give smooth model

$$\begin{bmatrix} L \\ D \end{bmatrix} \Delta m = \begin{bmatrix} r \\ 0 \end{bmatrix}$$

Many different approaches to global tomography

- P and S waves
- Surface Waves
- Normal Modes

- Finite Frequency Kernels
- Beginning Full Waveform Inversion using Adjoint Sources
- Models parameterized differently, regularization different

Comparison of Shear Wave Models

S40RTS – (Ritsema et al.,2011); SEMUCB_WM1 – (French&Romanowicz, 2014); S362ANI+M (Moulik&Ekstrom, 2014)

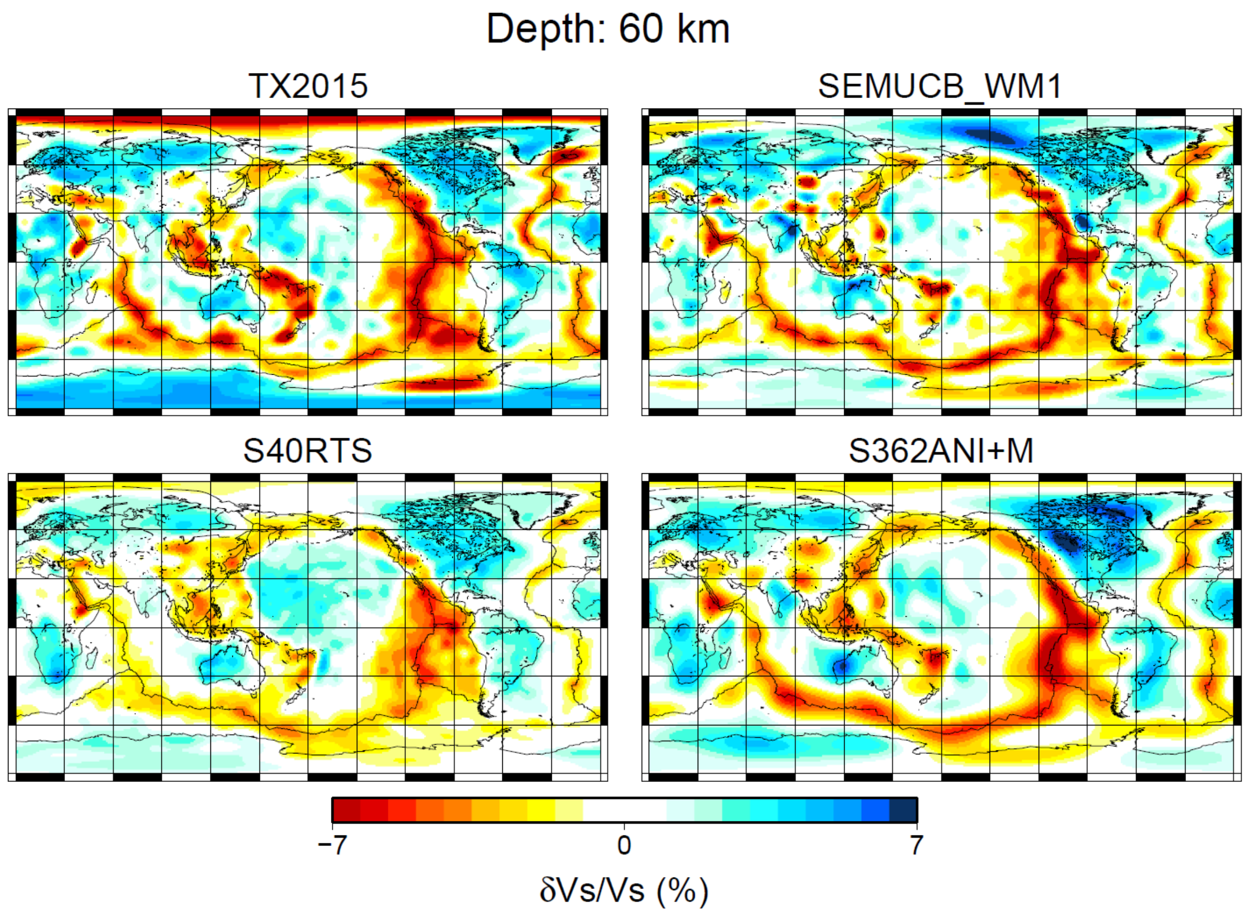

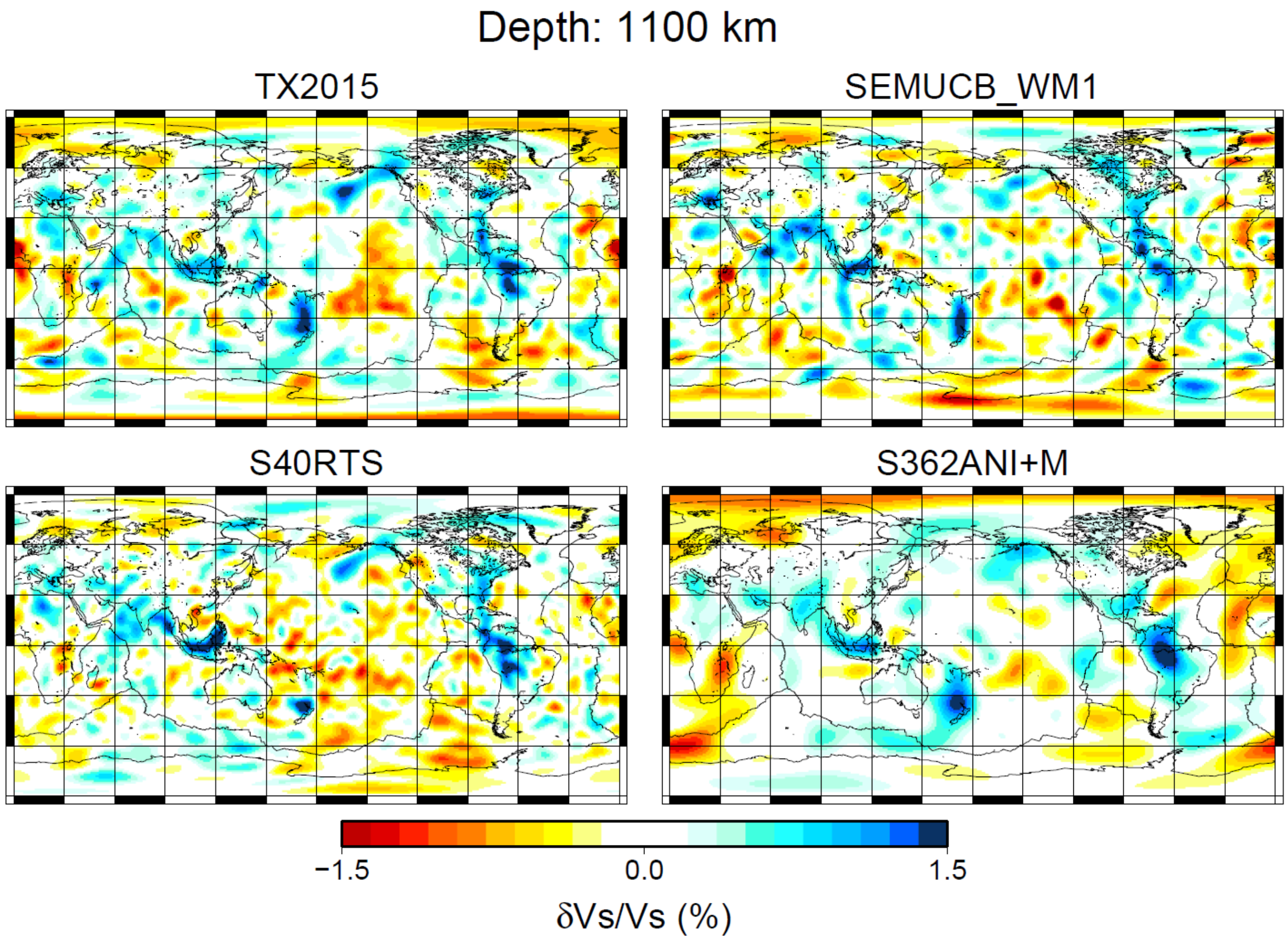
Depth: 1100 km
TX2015
SEMUCB_WM1
S40RTS
S362ANI+M
−1.5
0.0
1.5
δVs/Vs (%)

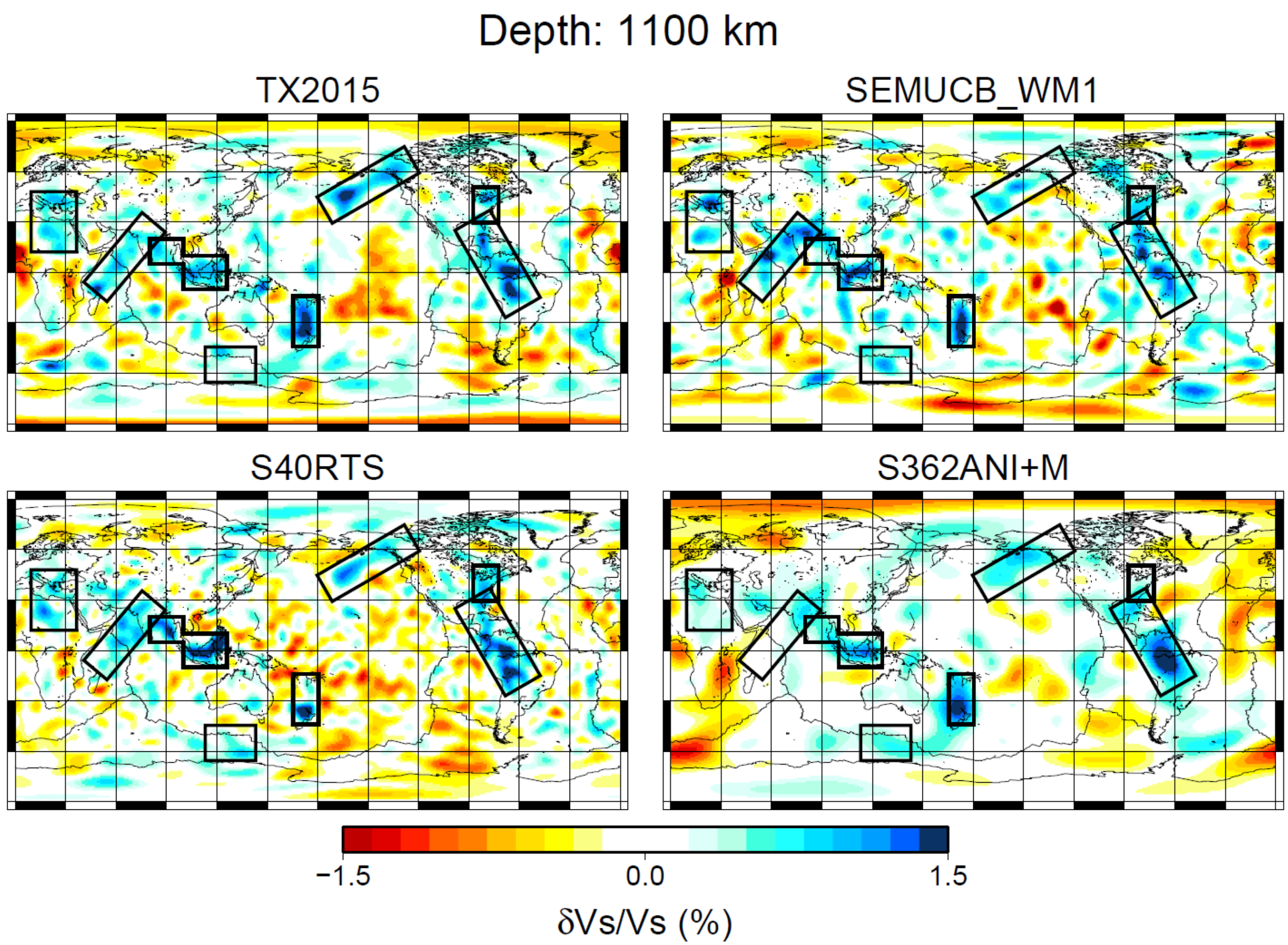
Depth: 1100 km
TX2015
SEMUCB_WM1
S40RTS
S362ANI+M
−1.5
0.0
1.5
δVs/Vs (%)

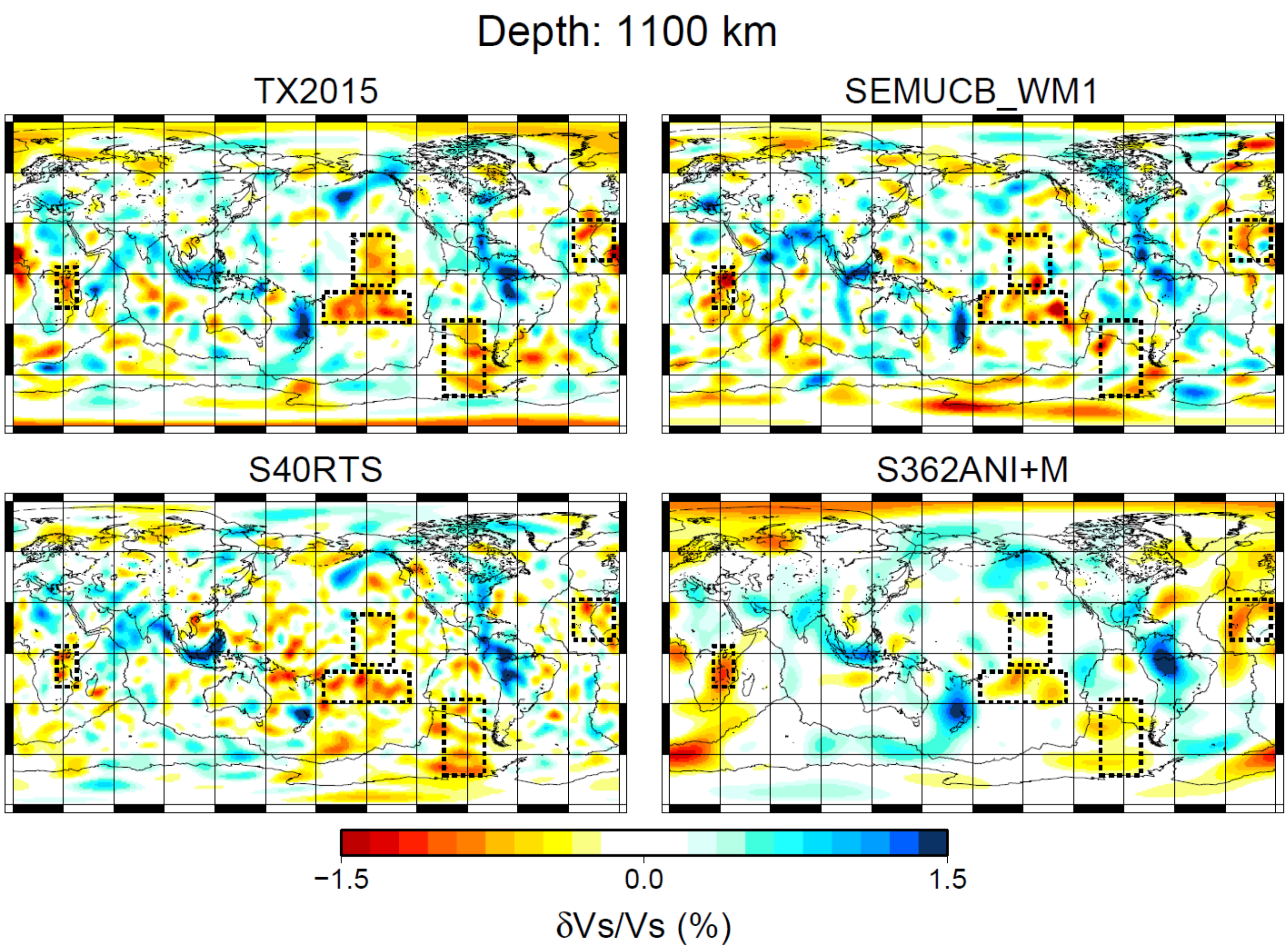
Depth: 1100 km
TX2015
SEMUCB_WM1
S40RTS
S362ANI+M
−1.5
0.0
1.5
δVs/Vs (%)

Different models use different data, smoothing weight, theory.
Large scale structures are similar but vary in detail

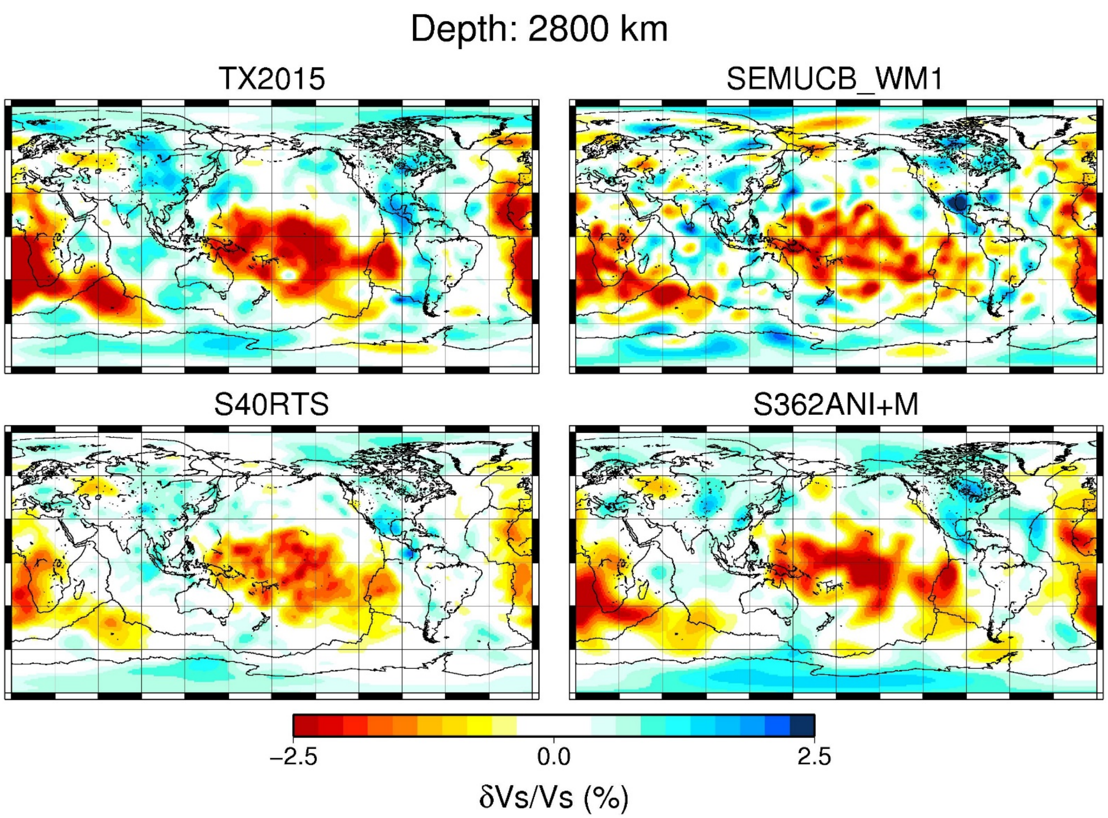

2800 km depth:

- Large scale strong slow velocity beneath Pacific, Africa

Large Low Shear Velocity Provinces (LLSVP)

TX2015: (Lu et al. 2016)
SEMUCB_WM1: (French and Romanowicz 2015)
S40RTS: (Ritsema et al. 2011)
S362ANI+M: (Moulik and Ekstrom 2016)

Interpretation of seismic tomography in terms of composition and dynamics difficult
Mapping density anomalies can help distinguish between thermal and chemical heterogeneities but constraining density is challenging using seismic observations alone

- Ishii and Tromp (1999), Lau et al. (2017) report anomalously high density within the African LLSVP using Earth's free oscillation, tidal tomography
- Koelemeijer et al. (2017) report the African LLSVP is buoyant using free oscillation data
- Density structure derived using seismic data alone is not reliable (Kuo and Romanowicz (2002)

Use Geodynamic Constraints.

Geodynamic observables related to mantle density are:

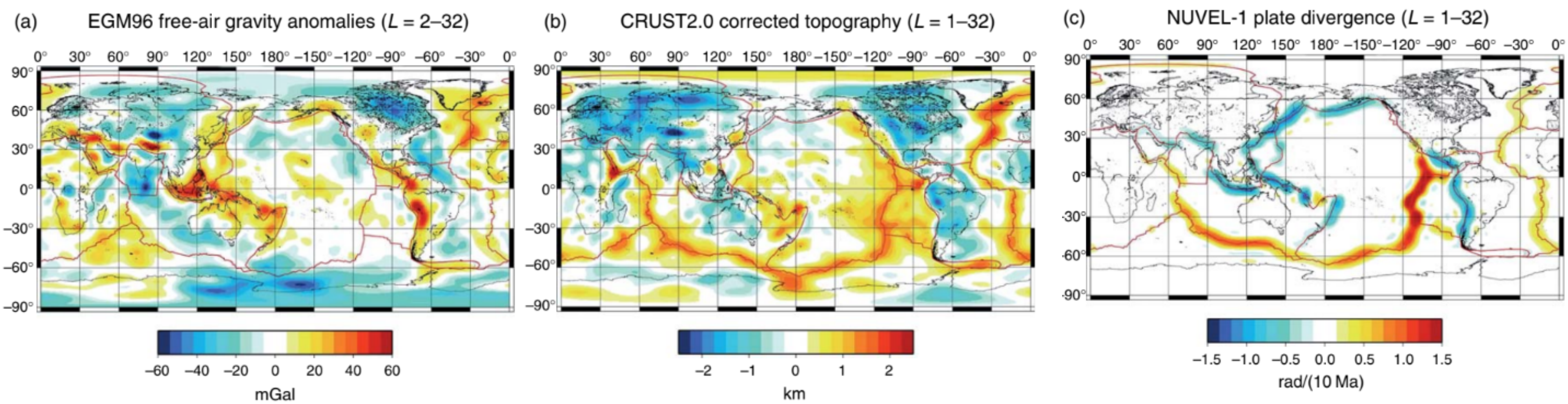

Free air gravity:
Gravity field of the earth determined by EGM96 potential field (Lemonie et al. 1998)

Dynamic topography:
Topography after taking out contribution from varying crustal thickness, caused by density anomalies in the mantle (Forte and Perry 2000; Laske et al. 2013)

Plate divergence:
Coupled with mantle flow beneath, mantle flow is determined by mantle density structure (DeMets et al. 1990)

Free-air gravity, surface dynamic topography, and plate divergence have been expanded up to spherical harmonic degree 32 (corresponding to ~1200 km wavelength)
(Forte 2007)

Geodynamic observables can be linearly connected to density anomalies in a dynamic mantle

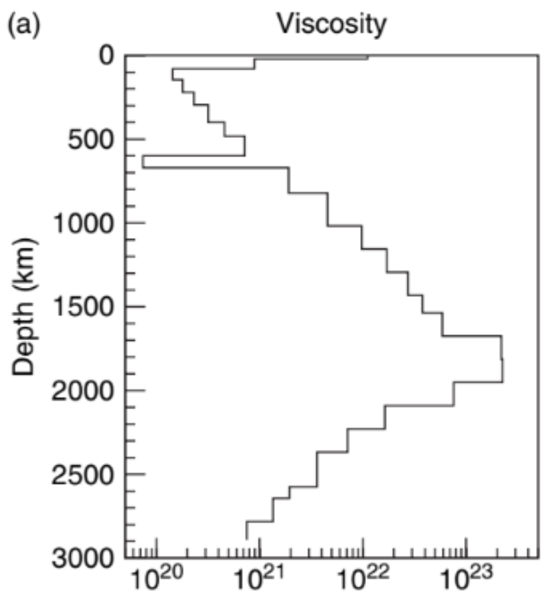

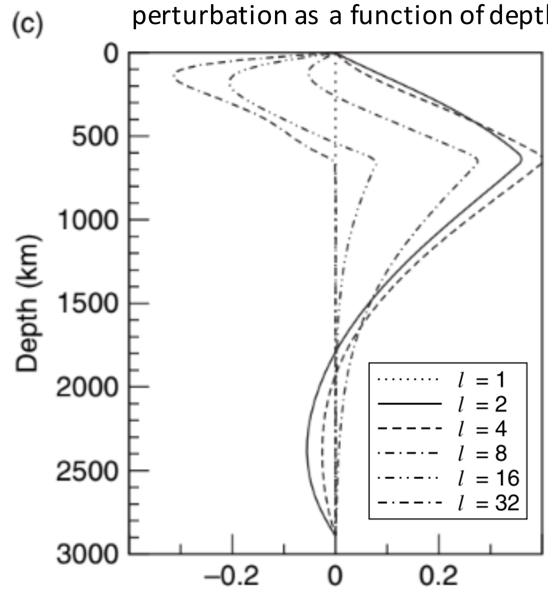

(Forte 2007)

Assuming a known viscosity model:

- The sensitivity of geodynamic observable to mantle density depends on the wavelength of the observable
- The same density anomaly at different depths may have opposite impacts on geodynamic observables

$$G\Delta\rho = u$$

G depends on viscosity!

The sensitivity matrix for geodynamic observables depends on the variation of viscosity as a function of depth – average radial viscosity profile in Earth is still uncertain

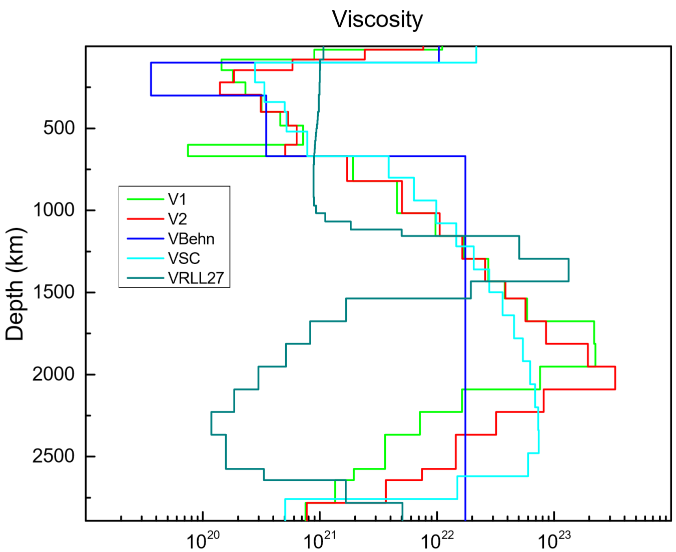

V1: Mitrovica and Forte (2004);
V2: Forte et al. (2010);
VBehn: Behn et al. (2004);
VSC: Steinberger and Calderwood (2006)
VRLL27 Rudolf et al. (2015)

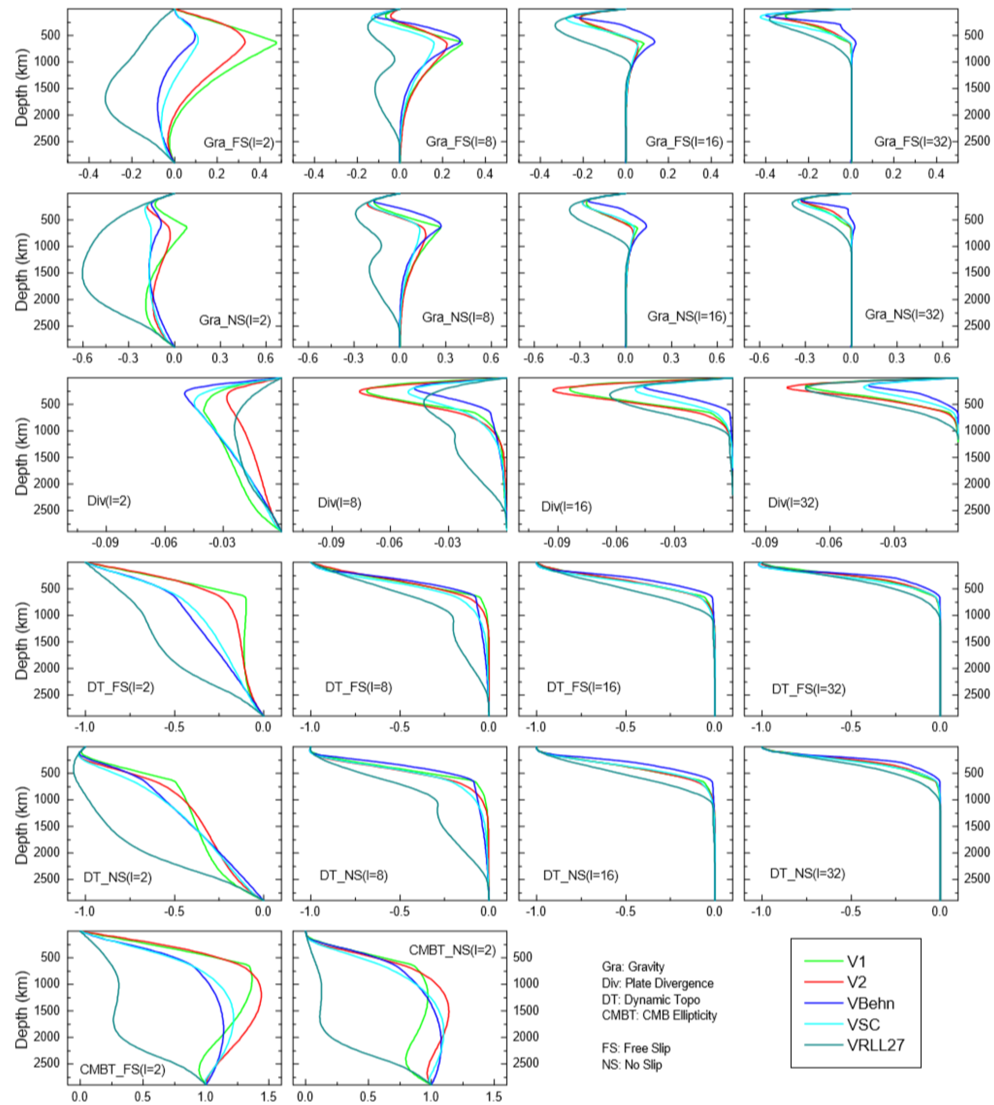

Assuming velocity anomalies are caused by temperature, density anomalies can be derived by scaling tomography model – but fit to geodynamic data is bad for 5 viscosity models tested

	Variance Reduction				
	V1	V2	VBehn	VSC	VRLL27
Gravity	-125.2%	-65.8%	-86.1%	-77.3%	-1805.8%
Plate Divergence	-117.9%	-12.3%	49.0%	50.7%	-63.3%
Dynamic Topo	-19.3%	-14.4%	-31.3%	-46.4%	-301.5%
CMBT (percent err)	112.0%	166.4%	256.2%	250.4%	213.1

Seismic sensitivity matrix

3-D seismic slowness perturbation

$$L\Delta m = r$$

Seismic residual

Geodynamic sensitivity matrix

$$G\,\Delta\rho = u$$

3-D Density perturbation

Geodynamic data

Density to velocity scaling factor from mineral physics

$$G(R_{\rho/Vs}\Delta m) = u_{pre}$$

$$VR = \left[1 - \frac{\sum_l \sum_{m=-l}^{+l} (O-P)_l^{m*} (O-P)_l^m}{\sum_l \sum_{m=-l}^{+l} O_l^{m*} O_l^m}\right] \times 100\%,$$

Seismic sensitivity matrix

Geodynamic data weight

Geodynamic sensitivity matrix

Smoothing matrix

$$\begin{bmatrix} L \\ \omega G\left(R_{\rho/S}\right) \\ D \end{bmatrix} \Delta m = \begin{bmatrix} r \\ \omega u \\ 0 \end{bmatrix}$$

Seismic data

Geodynamic data

(Simmons et al. 2009)

3-D seismic slowness perturbation

Density-velocity scaling factor

Correction for craton: $corrected\ R_{\rho/S} = R_{\rho/S} + k\Delta Vs$

Correction factor to be determined

Velocity perturbation from seismic tomography

Thermal density model: $\Delta\rho_{thermal} = R_{\rho/S}\Delta m$

Determine the optimal weight for geodynamic data

$$\begin{bmatrix} L \\ \omega G(R_{\rho/s}) \\ D \end{bmatrix} \Delta m = \begin{bmatrix} r \\ \omega u \\ 0 \end{bmatrix}$$

Seismic sensitivity matrix

Geodynamic data weight

Geodynamic sensitivity matrix

Smoothing matrix

Density-velocity scaling factor

3-D seismic slowness perturbation

Seismic data

Geodynamic data

(Simmons et al. 2009)

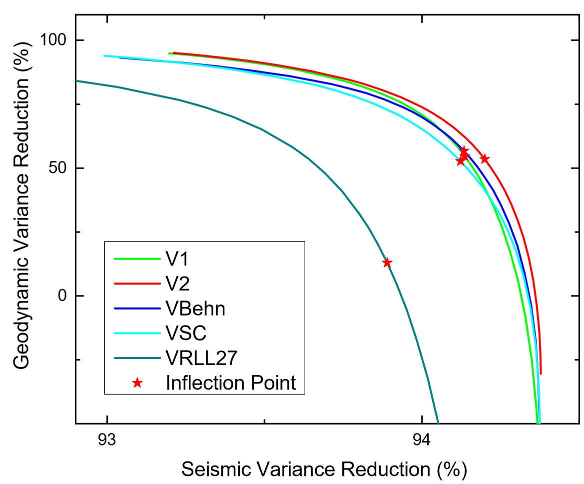

Increase geodynamic data weight until seismic data fit starts to drop

Much better fits to geodynamic data but still room for improvement

		V1	V2	VBehn	VSC	VRLL27
Gravity	Pure Seismic	-125.2%	-65.8%	-86.1%	-77.3%	-1805.8%
	Thermal- Joint	42.5%	32.0%	40.3%	30.8%	-121.1%
Plate Divergence	Pure Seismic	-117.9%	-12.3%	49.0%	50.7%	-63.3%
	Thermal - Joint	80.7%	80.0%	75.4%	80.7%	85.0%
Dynamic Topo	Pure Seismic	-19.3%	-14.4%	-31.3%	-46.4%	-301.5%
	Thermal Joint	52.8%	50.0%	46.9%	53.4%	48.6%
CMBT (percent err)	Pure Seismic	112.0%	166.4%	256.2%	250.4%	213.1%
	Thermal Joint	8.7%	8.1%	20.9%	23.6%	1.0%

Joint inversion keeps same fit to seismic data while improving geodynamic data fit significantly

Depth: 370 km

Depth: 2100 km

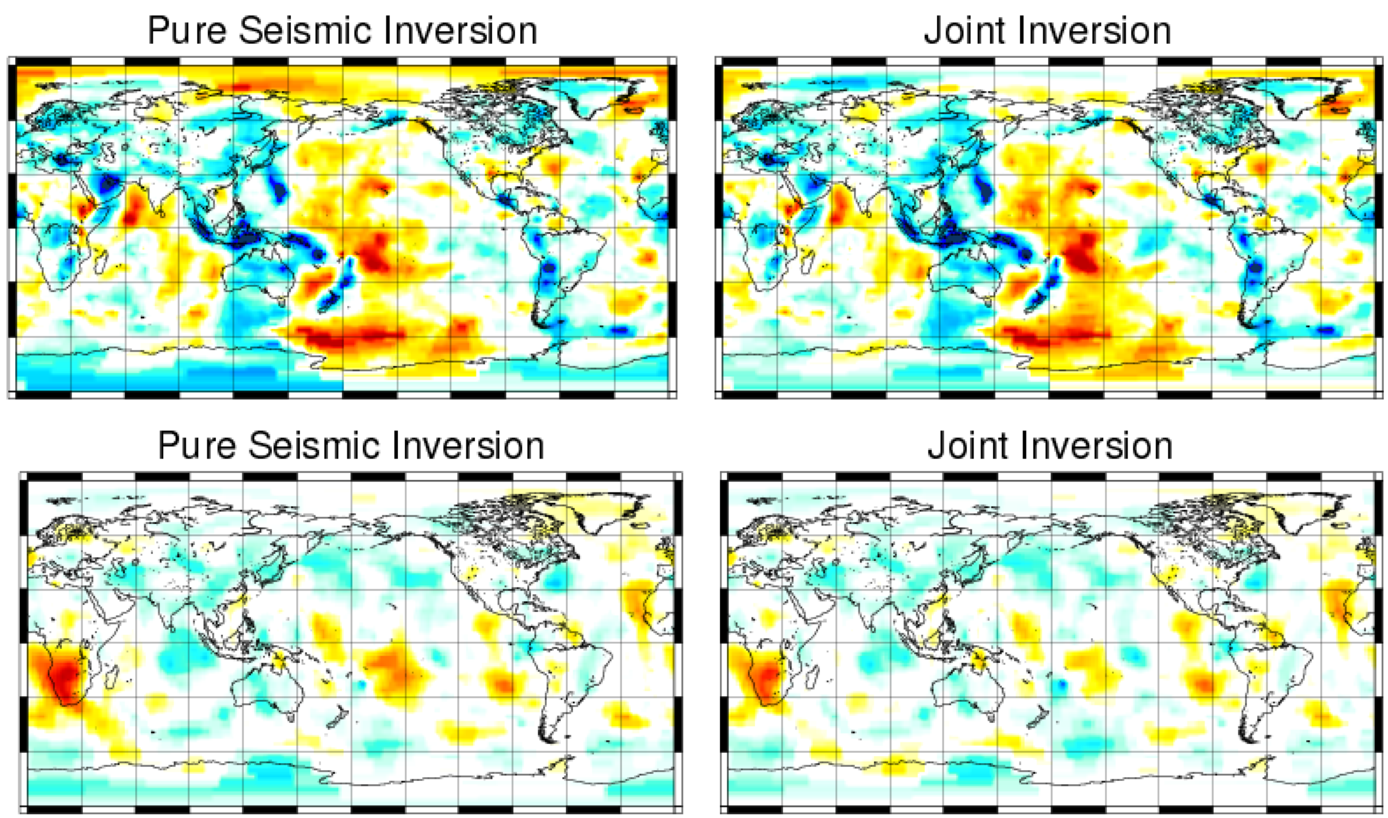

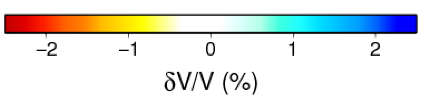

Invert for 3D scaling factor using geodynamic data assumed fixed velocity model

3-D seismic slowness perturbation from thermal inversion

$$\begin{bmatrix} G\,(\Delta m) \\ D \end{bmatrix} R_{\rho/S(3D)} = \begin{bmatrix} g \\ 0 \end{bmatrix}$$

Smoothing matrix (adjust weight to keep the roughness of density model to be the same as in thermal inversion)

3-D Density-velocity scaling factor

$$\Delta\rho_{thermal} = R_{\rho/S}\Delta m$$

$$\Delta\rho_{total} = R_{\rho/S(3D)}\Delta m$$

$$\Delta\rho_{chemical} = \Delta\rho_{thermal} - \Delta\rho_{total}$$

All geodynamic data can be well fit with 3D scaling factor

		V1	V2	VBehn	VSC	VRLL27
Gravity	Pure Seismic	-125.2%	-65.8%	-86.1%	-77.3%	-1805.8%
	Thermal- Joint	42.5%	32.0%	40.3%	30.8%	-121.1%
	Thermal+Chemical	93.6%	91.8%	80.4%	82.7%	64.7%
Plate Divergence	Pure Seismic	-117.9%	-12.3%	49.0%	50.7%	-63.3%
	Thermal - Joint	80.7%	80.0%	75.4%	80.7%	85.0%
	Thermal+Chemical	99.7%	99.6%	96.0%	97.8%	96.2%
Dynamic Topo	Pure Seismic	-19.3%	-14.4%	-31.3%	-46.4%	-301.5%
	Thermal Joint	52.8%	50.0%	46.9%	53.4%	48.6%
	Thermal+Chemical	80.1%	79.2%	71.2%	71.8%	74.1%
CMBT (percent err)	Pure Seismic	112.0%	166.4%	256.2%	250.4%	213.1%
	Thermal Joint	8.7%	8.1%	20.9%	23.6%	13.2%
	Thermal+Chemical	1.2%	0.5%	1.6%	0.2%	1.0%

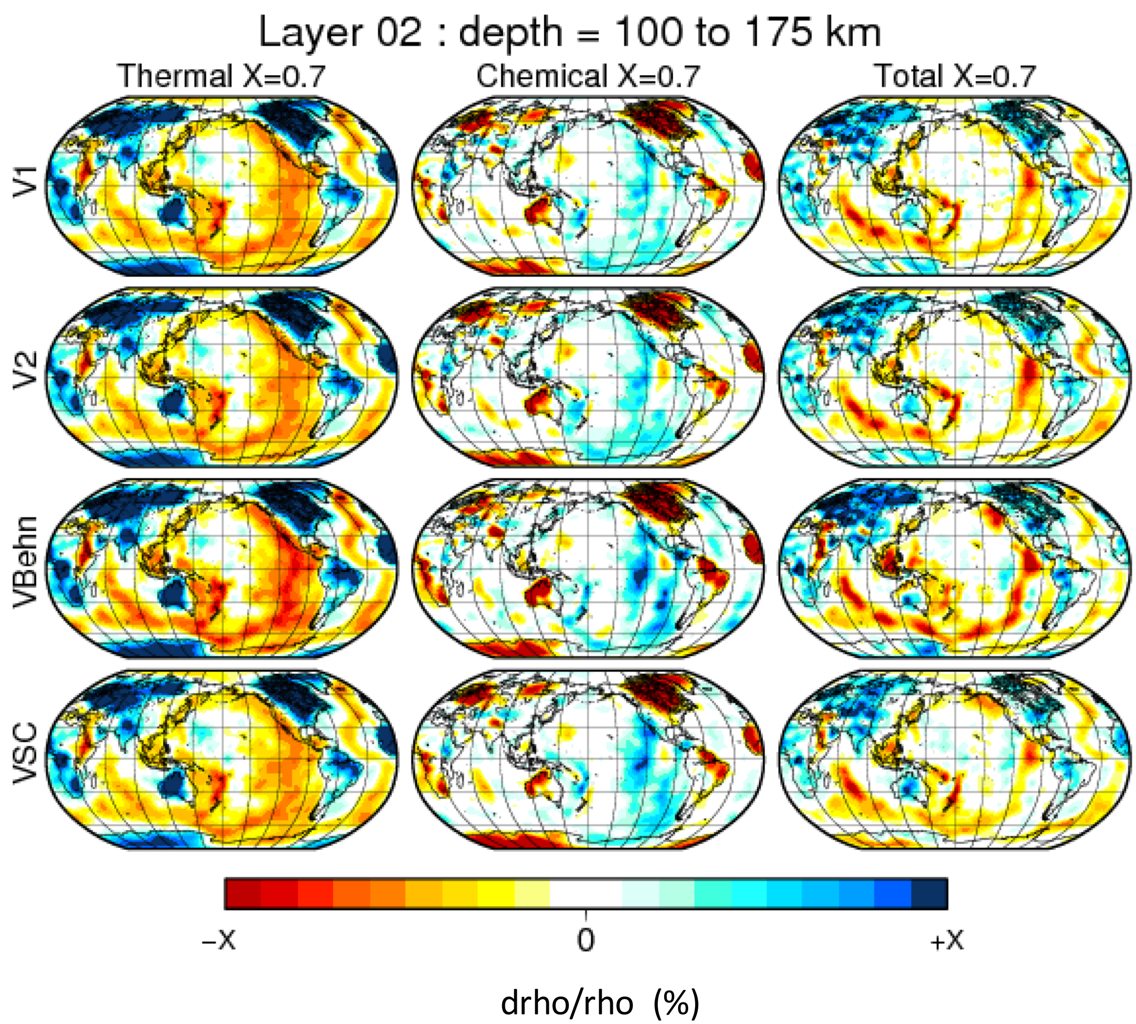

- Chemically distinct (less dense) craton root is required by geodynamic data

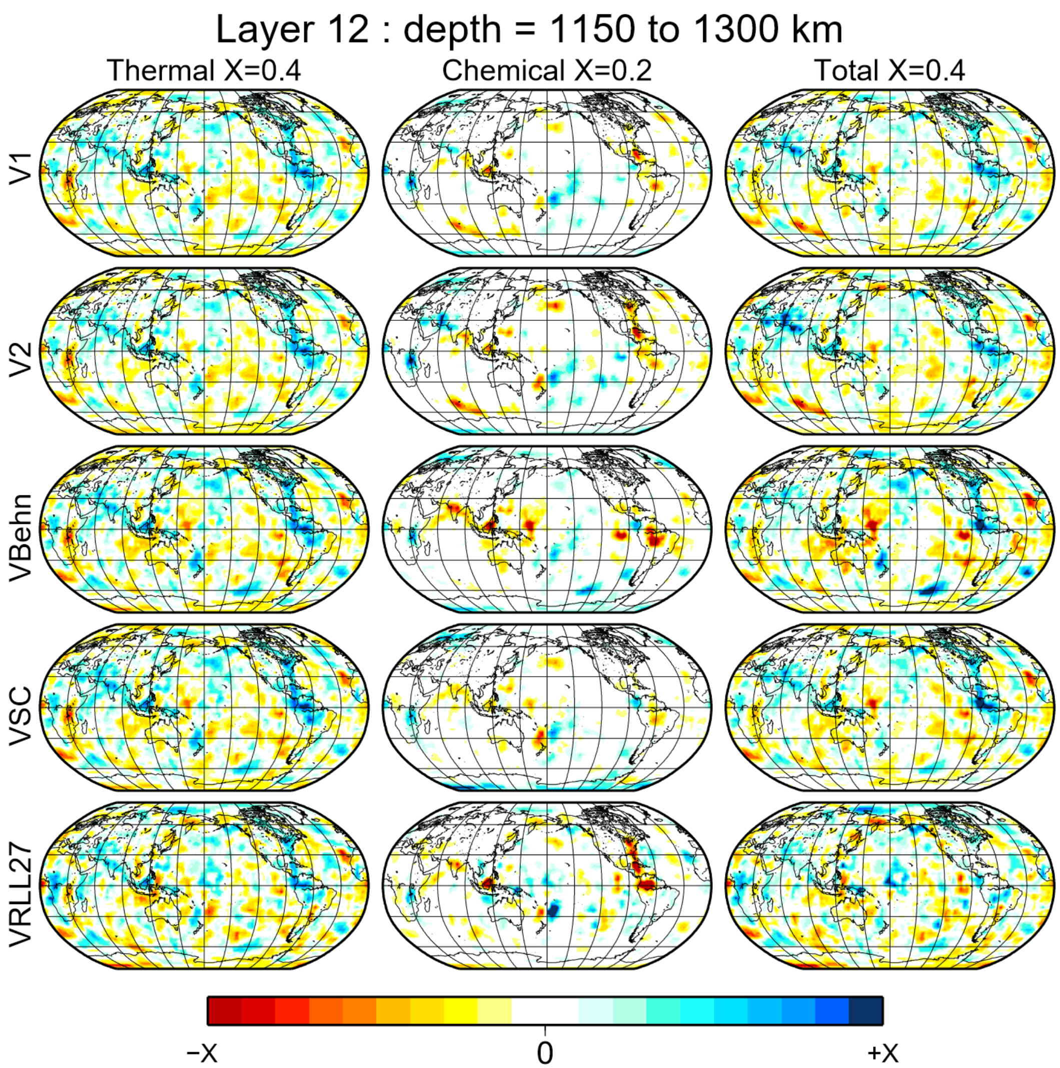

Little chemical heterogeneity in mid-mantle

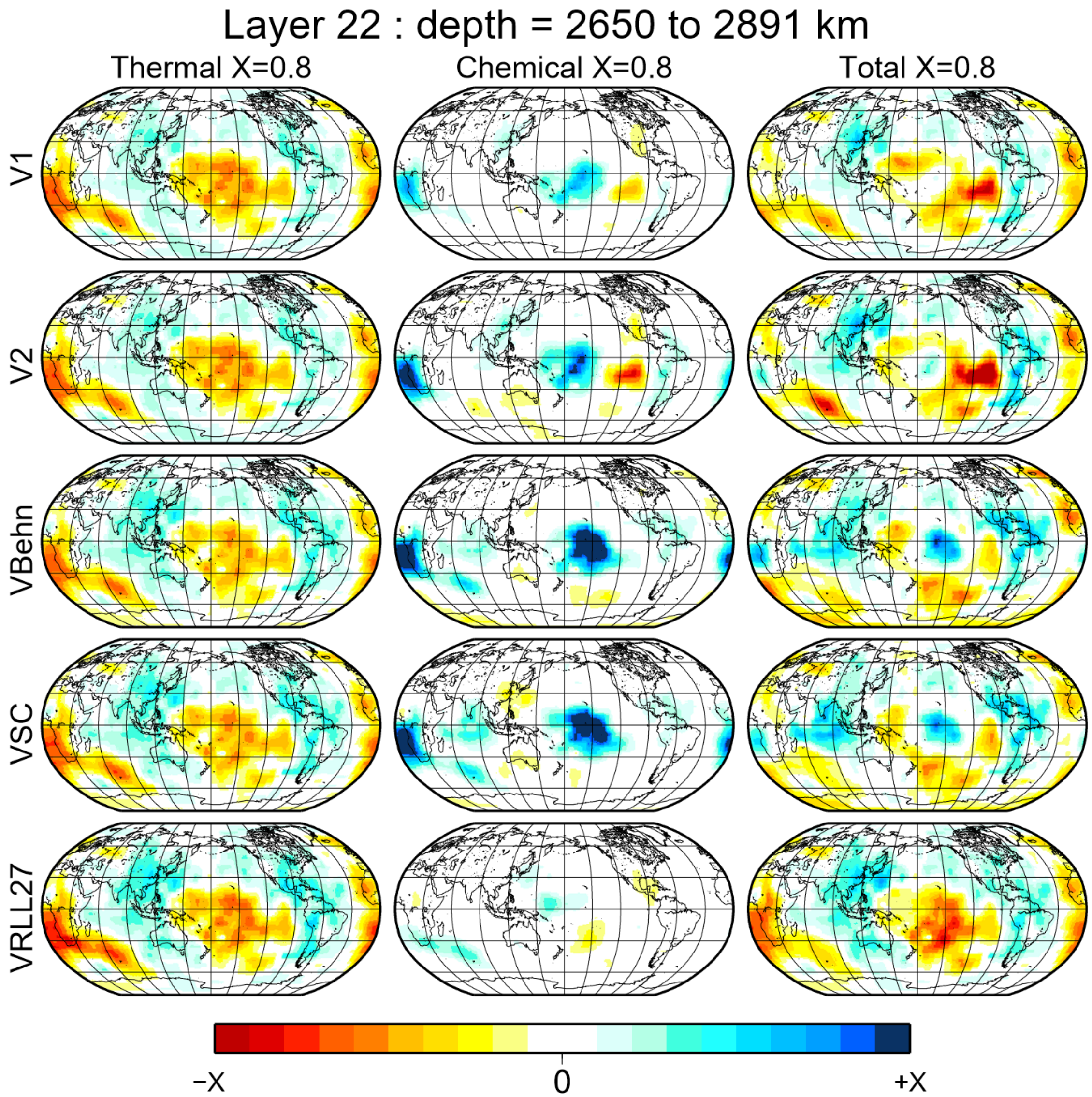

Chemically distinct LLSVP's detected at CMB

- Geodynamic data require less buoyant LLSVP
- The overall buoyancy of the LLSVP is neutral or negative!
- The edges of LLSVP are different from the interior of the LLSVP

Dense heterogeneity inside LLSVPs

- Chemically distinct LLSVP throughout whole depth, but overall denser LLSVP is only detected in the bottom ~400 km depth
- Most of Hotspots are correlated with buoyant regions at CMB

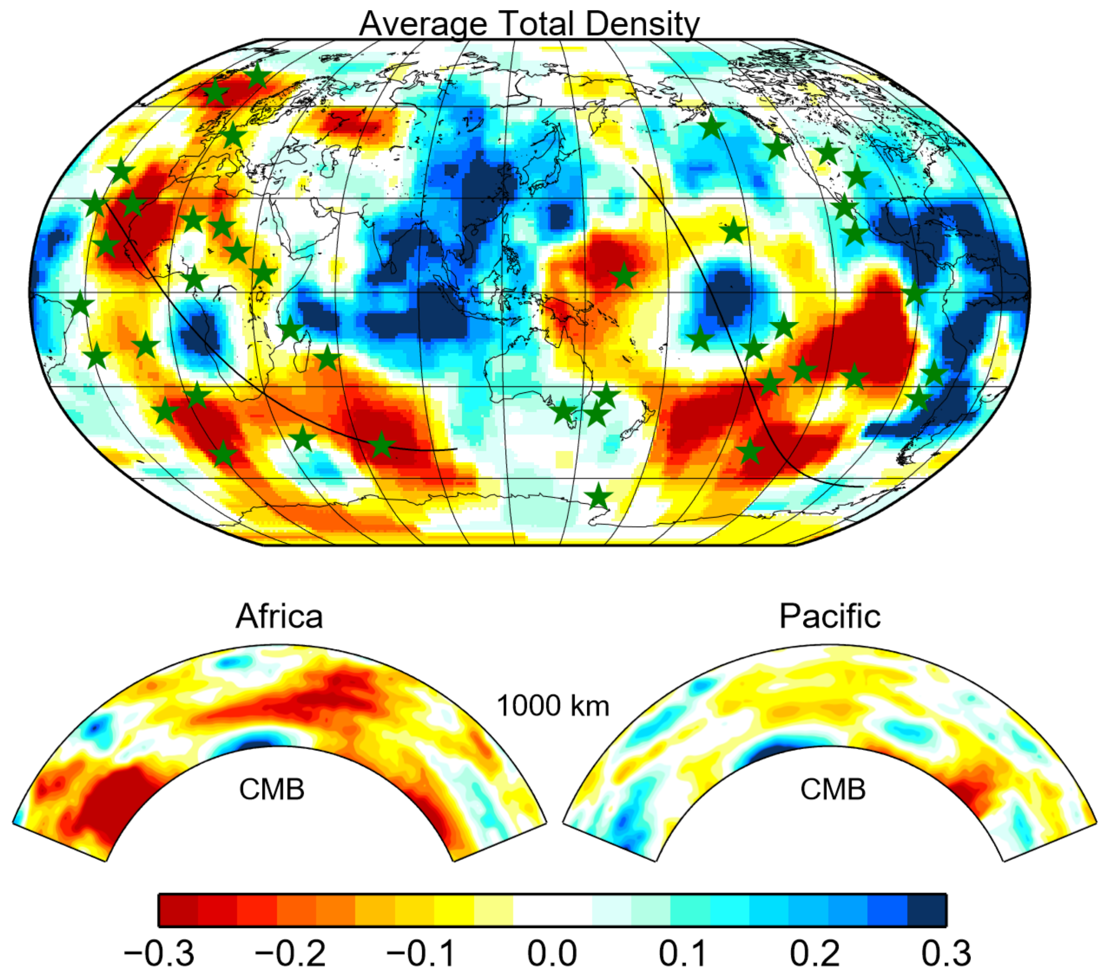

Hotspots locations: Steinberger 2000

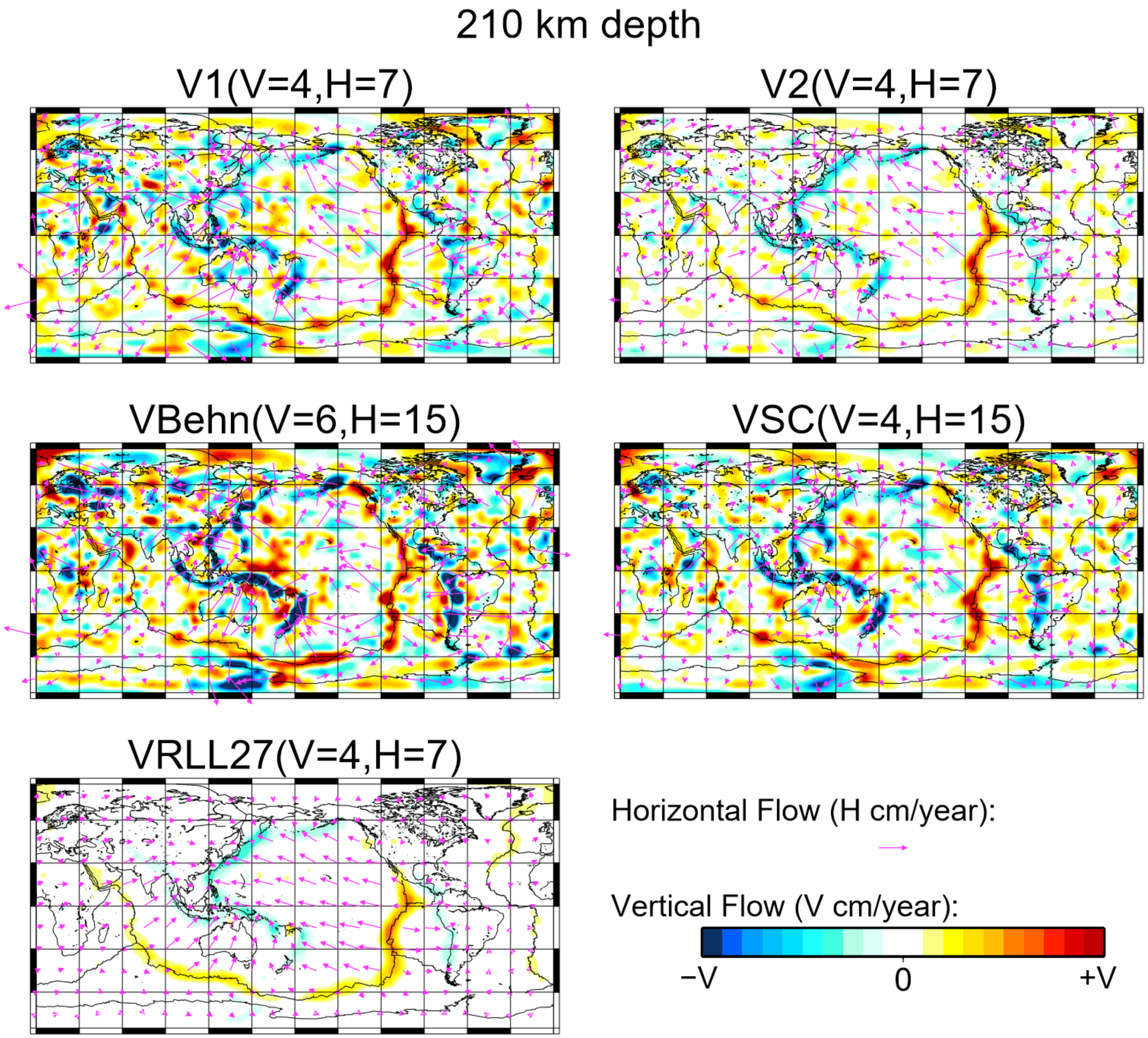

Mantle flow field can be calculated using density model and viscosity profile

- Downwelling in subduction regions and upwelling beneath mid-ocean ridges
- Flow velocities vary between models
- Opposite horizontal Flow directions beneath the caroline hotspot

Focused upwellings are found beneath many hotspot locations

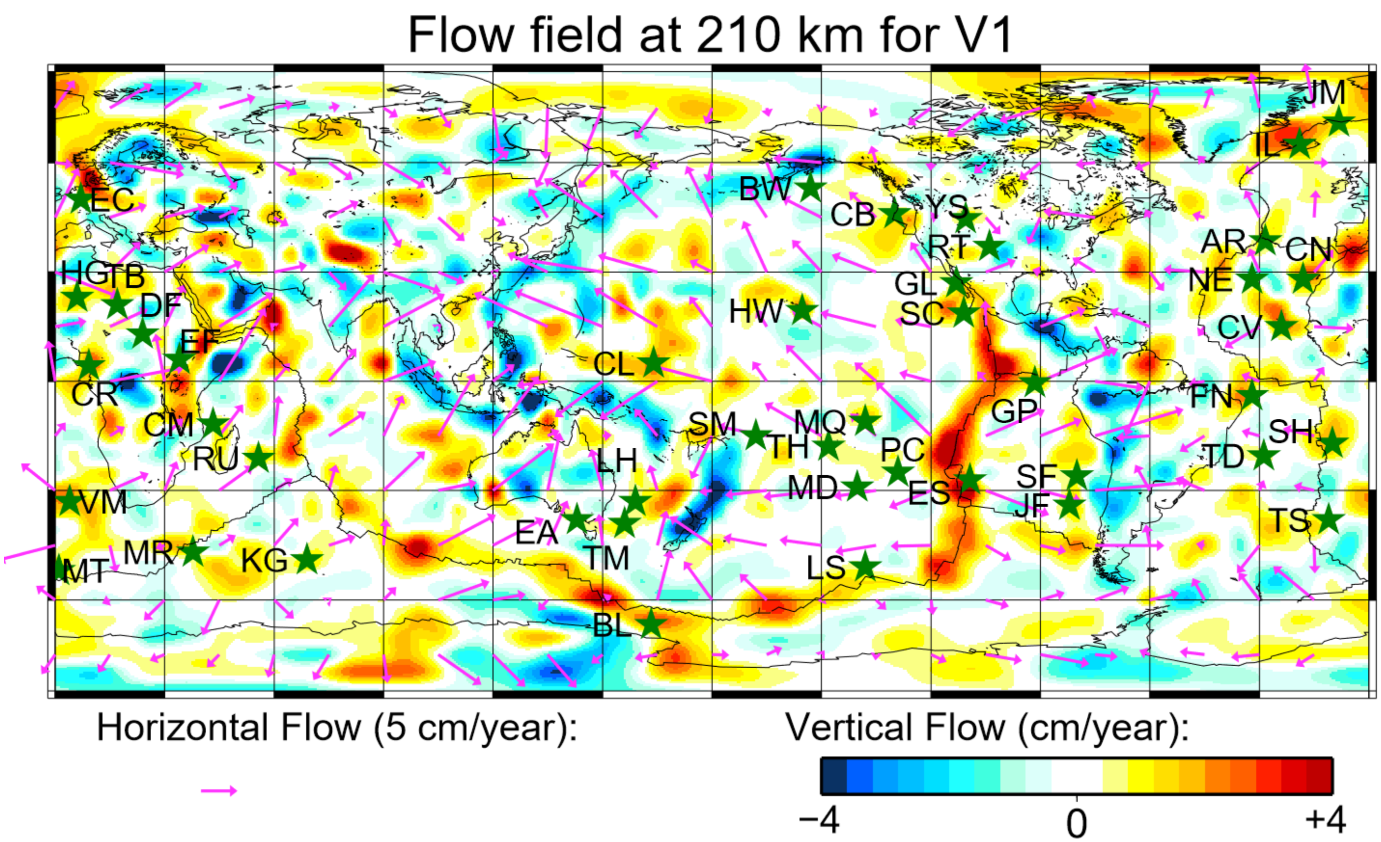

Hotspots locations:
Steinberger 2000

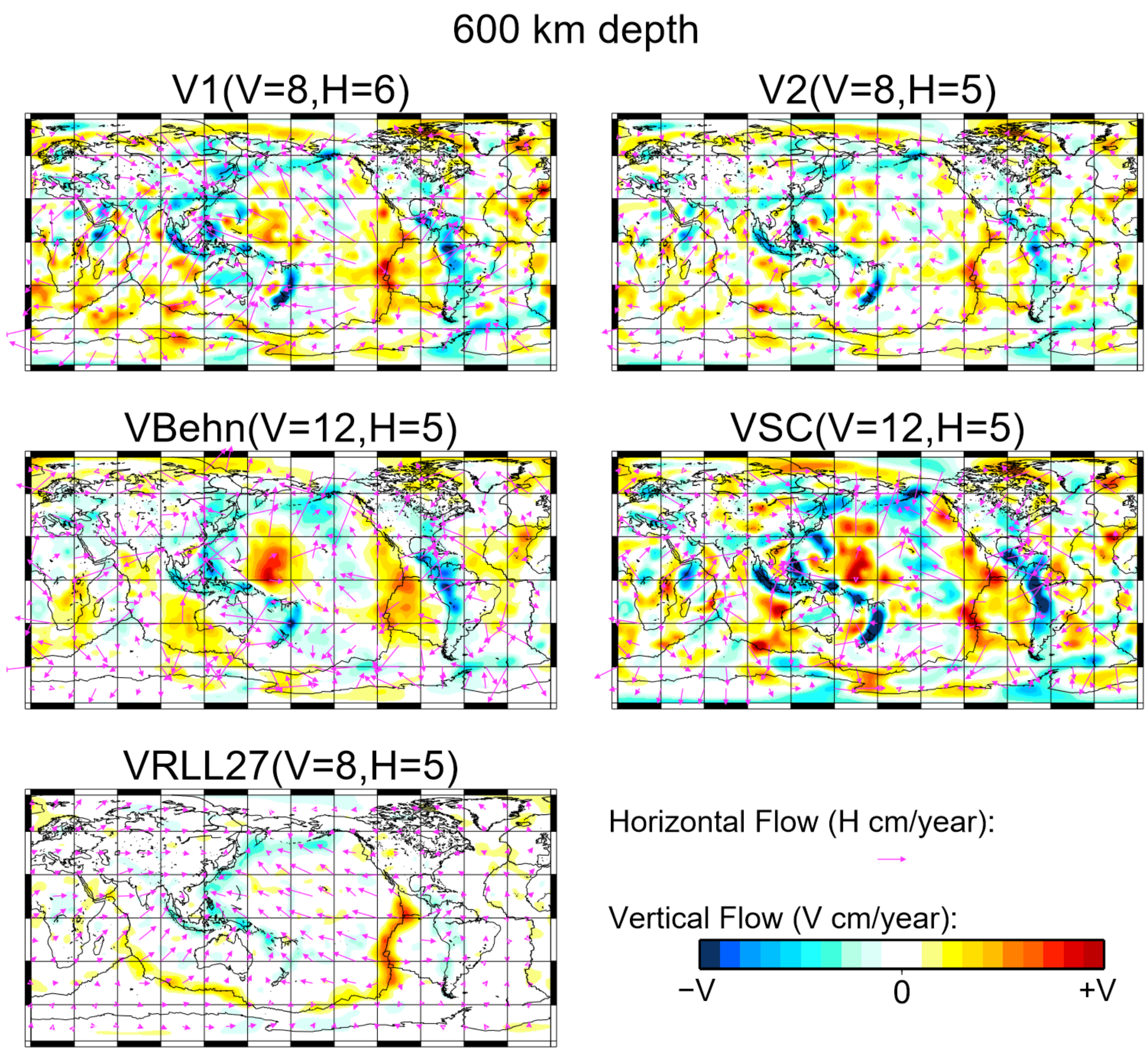

Mantle flow field can be calculated using density model and viscosity profile

- Flow models show more differences than at shallower depth
- Opposite horizontal Flow directions beneath the caroline hotspot

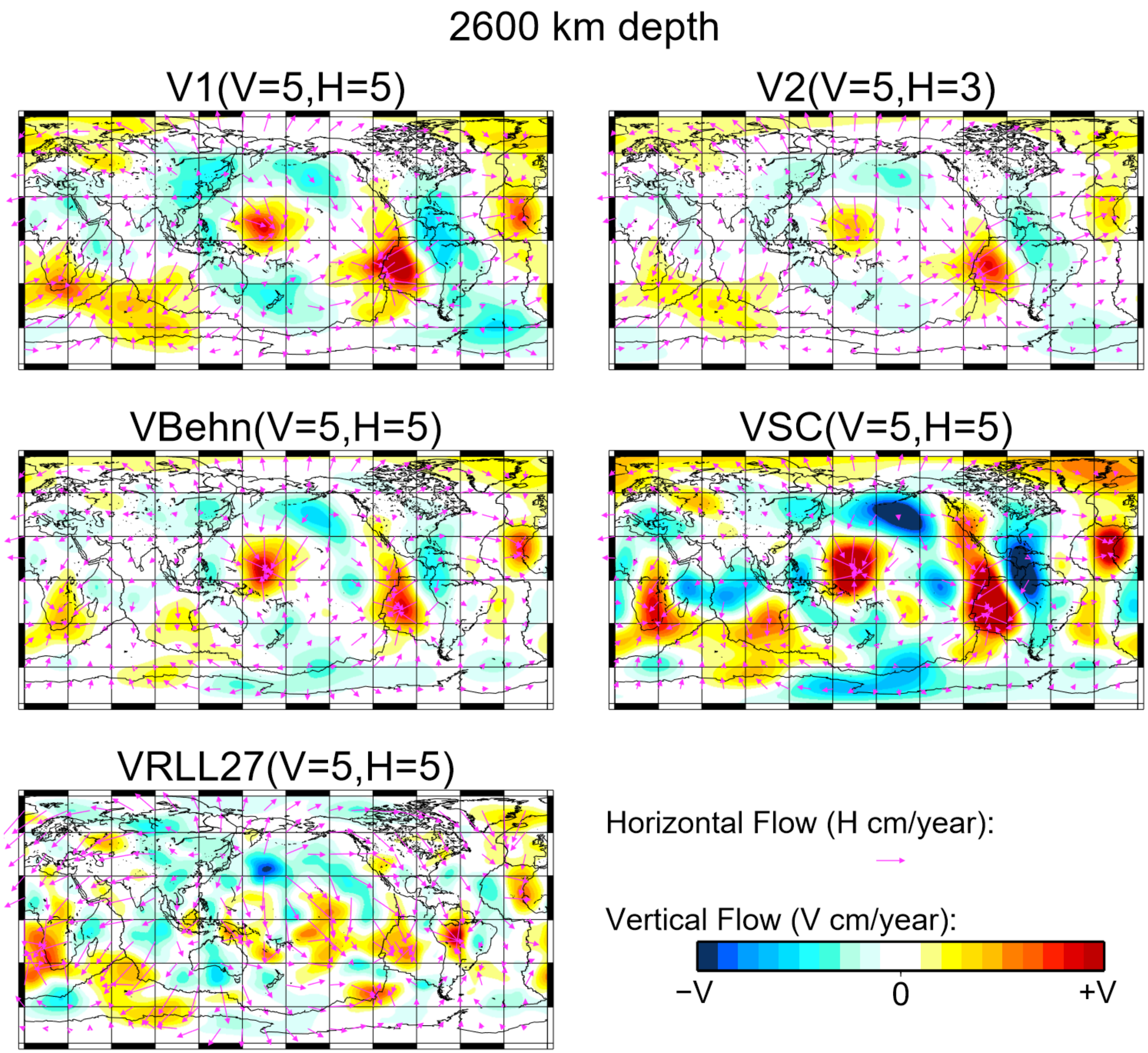

Five (six?) isolated deep upwellings under:

1) East Pacific Rise
2) Caroline hotspot
3) Cape Verde island
4) Southern Africa
5) Southern Indian Ocean
6) Maybe Iceland

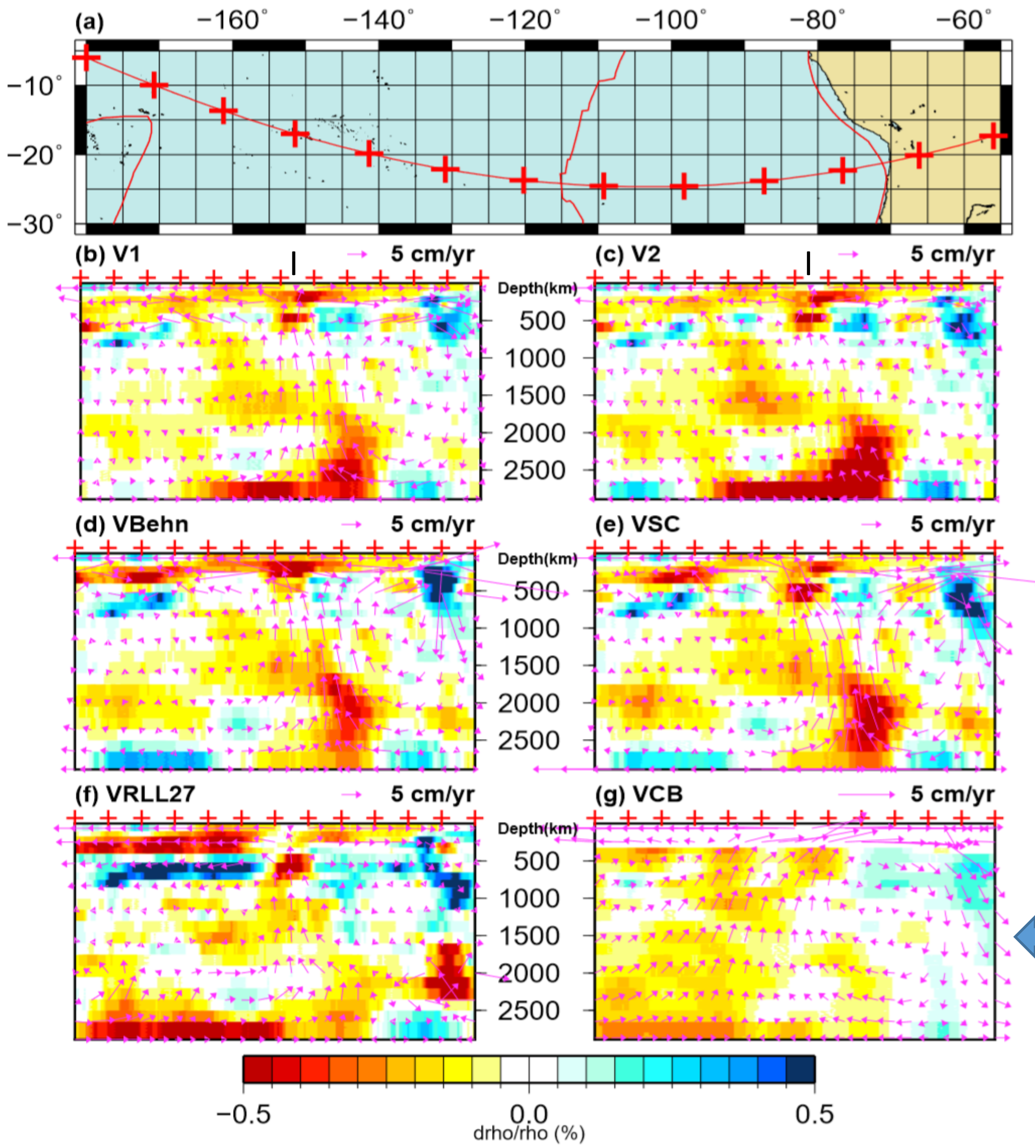

All the models from this study show a deep-mantle upwelling beneath East Pacific Rise (EPR), which is consistent with Rowley et al. (2016).

Density model is scaled from tomography model (Conrad and Behn 2010)

EPR ridge fixed through time (83Ma) in Indo-Atlantic hotspot reference frame – asymmetric spreading since 33.5 Ma (Rowley et al., 2016)

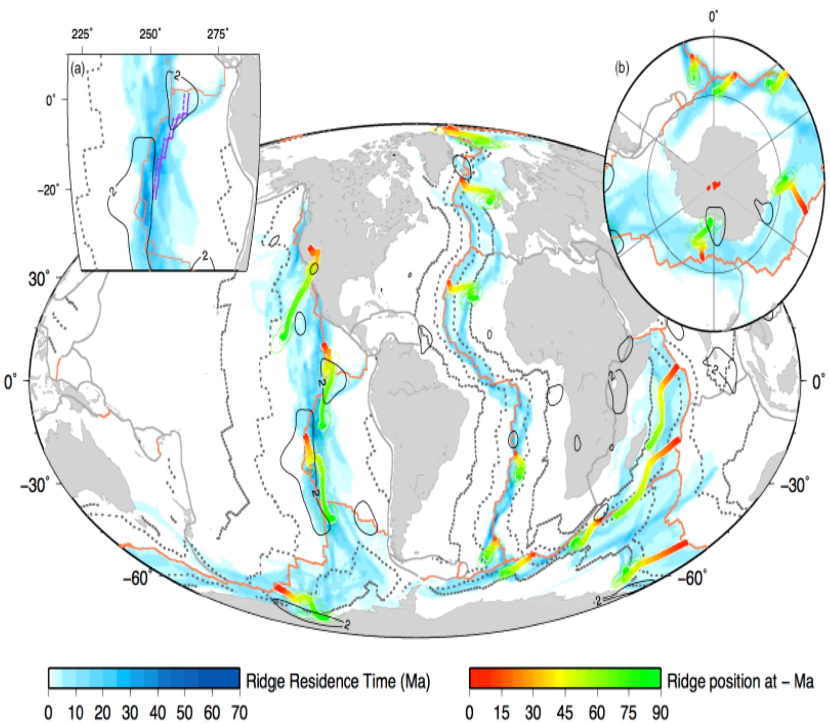

- Changes in subduction zone geometry (and age) in the western and eastern Pacific should have produced major changes in slab-pull and hence to motions of the EPR relative to the deeper mantle.
- Therefore, strong divergence rates and lateral stability of EPR since 83 Ma does not support the long-standing paradigm that lithospheric slabs (slab pull)
- Lateral EPR stability must instead be controlled by the strong whole-mantle upwelling directly below this ridge

Conclusion

- Joint inversion should be used to interpret seismic models in terms of temperature and density
- Surface boundary conditions important when modeling geoid, dynamic topography …..
- For the four viscosity models we test, chemical heterogeneities are required to explain geodynamic data but they are minor compared to thermal affects on density at most depths
- The cores of LLSVPs are chemically distinct from normal mantle, hotspots are correlated with the buoyant part of LLSVPs
- Different viscosity models give similar mantle flow patterns although the flow velocities vary a lot. Purely thermal scaling of seismic models results in significantly different deep mantle flow
- Current model predicts stronger influence of hot upwellings on surface tectonics than previously thought